MRS Advances © 2020 Materials Research Society
DOI: 10.1557/adv.2020.190

Influence of Controlled Cooling Rates During Thermal Processing of Ti 6% Al 4% V Alloys Using In-Situ Scanning Electron Microscopy

Genevieve A Kane,[1,2] M. David Frey,[2] Robert Hull,[1,2]

1Department of Materials Science and Engineering, 2Center for Materials, Devices and Integrated Systems, Rensselaer Polytechnic Institute, 110 8th Street Troy, NY, 12180

ABSTRACT

We describe experimental approaches to real time examination of the microstructural evolution of Ti 6%Al 4%V upon cooling from above the beta transus (~995 °C) while imaging in the scanning electron microscope. Ti 6%Al 4%V is a two phase, $\alpha+\beta$ titanium alloy with high strength and corrosion resistance. The $\beta \rightarrow \alpha$ transformation on cooling can give rise to different microstructures and properties through various thermal treatments. Fully lamellar microstructures, bi-modal microstructures, and equiaxed microstructures can each be obtained by accessing different cooling rates upon the final treatment above the beta temperature, each resulting in uniquely enhanced material properties.

Utilizing the capabilities of a heating/ tensile stage developed by Kammrath & Weiss Inc., are able to apply real-time imaging techniques in the scanning electron microscope to monitor the development of the microstructure. Annealing temperatures up to 1100 °C are attainable, with cooling rates ranging from 0.1 ° C per second to 3.3 °C per second. This has allowed us to directly observe the formation of lamellae at different annealing temperature/ cooling rate combinations to determine the lamellar microstructure width, separation, and colony size.

INTRODUCTION:

Ti 6% Al 4% V is a two-phase alloy comprised of α (hcp) + β (bcc) phases that is known for high strength and corrosion resistance, and has aerospace and

biomedical applications [1], [2]. The control of transformations between α and β through thermomechanical processing conditions allows control of the resultant mechanical properties.

Three primary characteristic microstructures are observed upon cooling from above the beta transus near 1000° C. 1) Lamellar microstructures occur when α precipitates form in the β matrix upon cooling, creating lamellar structures that are separated by the retained β in the grain. The overall microstructures comprise "colonies." Colonies are areas of α which have the same misorientation with relation to the β grain. The size of colonies and the number of lamellae therein depends on cooling rate, with faster cooling rates resulting in smaller colonies [3]. 2) Widmanstatten microstructures form at higher cooling rates, forming as elongated α precipitates. Precipitate growth can occur from the lamellar interfaces, and intersect each other forming a characteristic "basketweave" [4]. 3) At higher cooling rates, martensitic phase transformations can also occur creating both α', a hexagonal structure, and α'' which is orthorhombic [5].

Thermomechanical processing of Ti 6%Al 4%V involves multiple steps including material homogenization above the β transus, deformation and recrystallization in the $\alpha+\beta$ regime and further annealing at lower temperatures [6]. These hot working and heat treatment steps allow the material to undergo a transition from high temperature β to a lower temperature, two-phase $\alpha+\beta$ colony microstructure [7]. Heat treatments vary depending on the desired material properties. Properties such as yield strength, and fracture toughness will be a function of the size of the α grains, volume fraction and the microstructure[8], [9]. For example, to optimize strength, cooling rates below 2 °C/s will yield lamellar microstructures, with faster cooling leading to smaller colonies. This leads to an increased impediment of dislocation motion [10]. Fracture toughness can be optimized by producing a basketweave microstructure or lamellar microstructures[11], [12]. A material's ability to resist brittle fracture increases with the increase of lamellar structures and acicular (needle-like) microstructures. These are capable of influencing the crack path and causing further crack deflection, impeding crack growth more than the bi-modal microstructure [13], [14].

This paper describes the development of techniques that enable real time study of the evolution of microstructure in Ti 6% Al 4% V when cooling from above the β transus at cooling rates of ~3.3 °C/s (basketweave) and at 0.1 °C/s (lamellar microstructures). The ability to bring the sample above the β transus allows for homogenization of the microstructure into large β grains, and direct observation of the reintroduction of α lamellae into the β matrix upon cooling.

EXPERIMENTAL METHODS:

A heating-stressing-indentation stage from Kammrath and Weiss GmbH, is integrated with a Zeiss Crossbeam (dual focused electron and ion beam) instrument. The stage, Figure 1, is capable of heating to a maximum temperature of 1200° C. An

example radiative cooling curve is shown in Figure 1c. The radiative cooling rate is an average of around 3.3 ^{0} C/s in the temperature range 1100 – 500 ^{o} C, where most microstructural evolution is observed. Lower cooling rates (0.1 °C/s) are controlled through a proportional–integral–derivative (PID) controller.

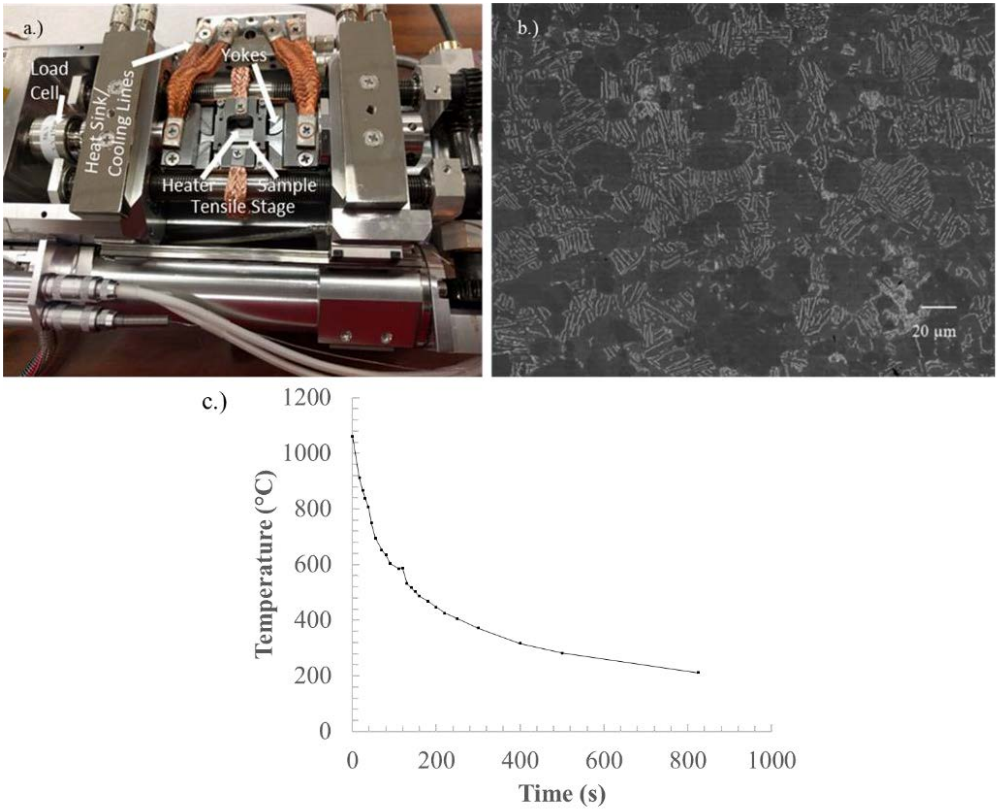

Figure 1 a.) Overview of the heating / stressing stage. b.) Secondary electron image of starting bi-modal microstructure of Ti 6%Al 4%V samples taken at 5 keV primary electron beam energy. c.) Example radiative cooling curve.

The stage is equipped to apply tensile loads up to 5 kN, corresponding to stresses up to about 1 GPa for our sample dimensions, with strain rates ranging from $1x10^{-3}$ s^{-1} down to $1x10^{-5}$ s^{-1}. However, all experiments described in this paper are with zero applied load. Samples of Grade 5 Ti 6%Al 4 %V are obtained from ATI specialty materials (https://www.atimetals.com/) and electrical discharge machined to required dimensions. The dimensions comprise a 24 mm gauge length, with a width of 2.5 mm and a final sample thickness of 1.5-1.6 mm after polishing and etching. After electrical discharge machining, the samples are mechanically ground using 15 micrometer abrasive, followed by a 60 nm colloidal silica polishing, and etch in Kroll's reagent for 6s. The expected starting micro-structure of equiaxed α grains with regions of mixed phase lamellar microstructure is seen in Figure 1b. The lighter contrast of β is

attributed partially to the different secondary yield of the α and β phases, and also to the topography associated with the lamellae due to different etch rates between α grains and lamellar microstructure.

Relatively long working distances of 25 mm are used in the SEM during imaging due to the stage geometry and the need to minimize the effects of stage heating on the electron/ion columns and detectors. With this working distance we are able to attain to approximately 10 nm resolution with an incident electron beam energy of 20 keV. Due to a starting average grain size that is tens of micrometers in size, experiments target relatively low magnifications and large fields of view to view a statistically significant number of grains – field widths of 60 µm, 300 µm, and 2 mm were typically employed. Secondary electron (SE) images were taken using either 20 keV primary electron beam energy to optimize image resolution, or 5 keV to optimize contrast.

During sample heating, ramp rates of 100 °C per minute are used for the PID controller, to the maximum controller temperature of 1200 °C in all experiments. Thermocouple readings are taken from the top surface of the heater cover, where a type R thermocouple is inserted into the heater cap ("Heater TC"). In addition to this, a type R thermocouple is spot welded to the top surface of the sample to give the temperature close to the area of viewing ("Sample TC"). At the 0.1 °C/s cooling rates, SE images can be recorded during a temp. change of ~ 10 ^{o}C. These cooling rates encompass the conditions for formation of lamellar and basketweave microstructures [15], [16].

RESULTS:

A salient result of our observations is that a periodic surface topography forms in all samples heated to near or above the beta transus, and persists – even amplifies – during subsequent cooling to room temperature. Figure 2 shows the evolving microstructure during an experiment employing the radiative cooling rate. Figure 2a and 2b show the topography in the β grains after sample heating at 1060 °C for 40 minutes, with the direction of the topography varying from grain to grain, presumably depending on the grain orientation. Figure 2c and 2d are imaged upon cooling to below 200 °C, where the basket weave structure has developed in each grain during cooling.

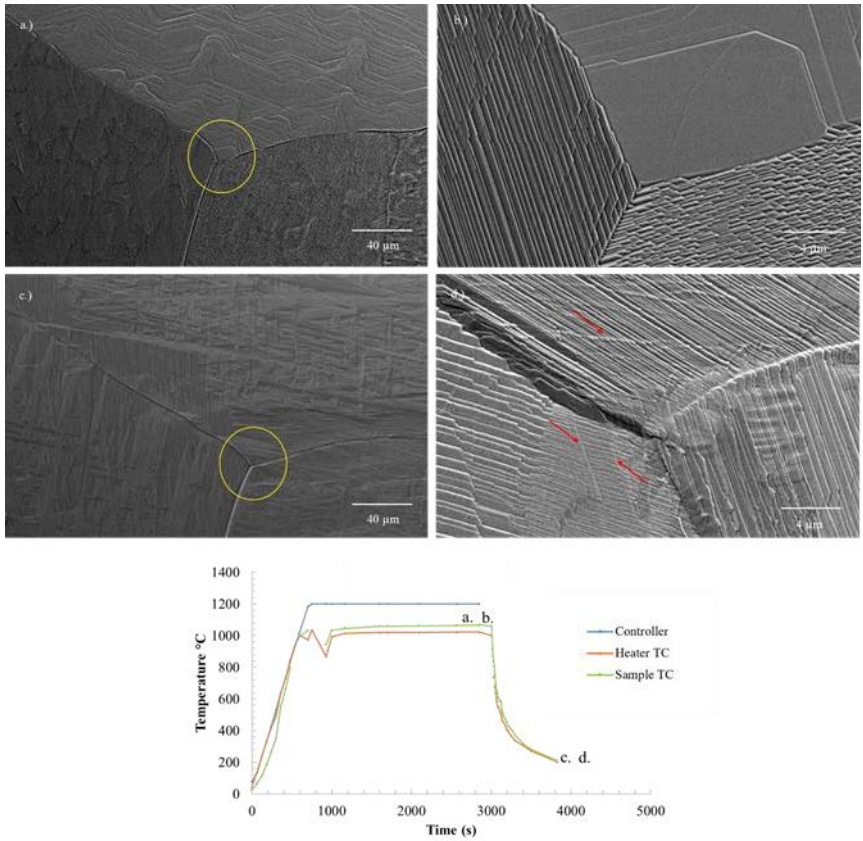

Figure 2: Microstructure evolution at a) Triple junction after 40 mins at 1060 °C imaged at 20 keV primary electron beam energy b) post cooling microstructure at triple junction imaged at 20 keV c) triple junction examined at higher magnification at 1060 °C imaged at 5 keV primary electron beam energy d) microstructure of triple junction post cooling imaged at 5 keV primary electron beam energy. Temperature -time curve for this experiment included.

Figure 3 correlates atomic force microscopy (AFM) and SEM images of the periodic surface topography. To our knowledge this topography has not been previously reported in the literature. This may be because in ex-situ studies that examine microstructure after the processing cycle, this surface topography would be typically removed by sample polishing and etching prior to imaging. The amplitude of the topography from our AFM studies is of the order of 100 nm, which would be removed during such procedures. No observable α case was found in these experiments, nor do we anticipate such formation based on the work of Brice et al, where the formation of a 40 µm and 80 µm α case in ambient air furnace studies was shown at temperatures of 950 ° C for 25 hours and 50 hours respectively [17]. Performing our heat treatments in vacuum of 10^{-5} Torr for less than 1 hour would thus greatly restrict α case formation.

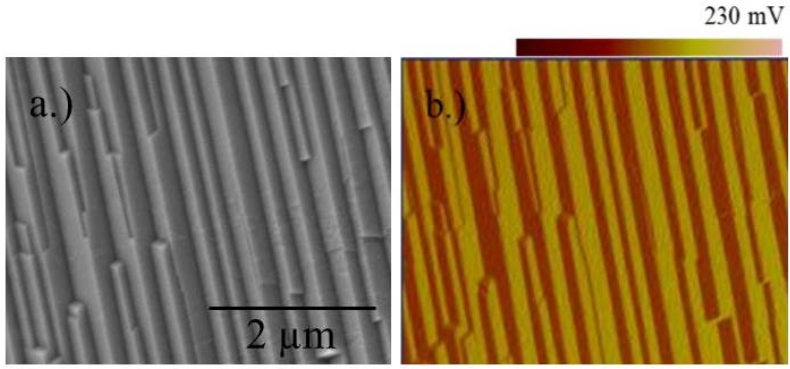

Figure 3: a) SEM Image of surface topography following sample heating and cooling taken with 5 keV primary electron beam energy. b) Amplitude scan from AFM from corresponding area.

The period of the surface topography from Figure 3 is around 300 nm. In areas where the lamellar structure co-exists with this topography, the period increases, by a factor 2-3x.

To further investigate how the lamellar microstructure evolves, a sample was annealed to 1100 °C and then cooled at 0.1 °C/s until the lamellar structure began to form starting at 946 °C (as measured by the sample thermocouple) as seen in Figure 4a. At this point, the lamellae ranged from around 40 – 160 µm in length. Over the course of two minutes at 946 ^{o}C, the length of the lamellae approximately double, as seen in Figure 4b. Notably, significant growth did not occur after the first three minutes for these lamellar structures, despite the sample being held at 946 ^{o}C for 45 minutes (sample temperature varied by less than 5 °C during this hold period). Figure 4c and 4d show the sample after this holding period. The lamellar microstructure remained 3.5 – 7 µm in width during the holding period, and remained similar in length to those shown in Figure 4b at around 80 – 300 μm. Figure 4d shows the aforementioned periodic topography within the grain at higher magnification, and also shows the change in direction of the topography in the neighbouring grain. It is again noted that this topography changes periodicity in regions where the lamellar structure co-exists with it. Figure 4e shows the sample cooling to 800 °C at 0.1°C/s, where there is a significant widening of the existing lamellae to 6 – 13.5 µm in width. Again, there is no significant change in length. Additional lamellae do begin to develop and grow upon further cooling, but the previously formed lamellae remain stagnant in length. When the sample reaches 445 °C during cooling, the originally observed lamellar structures continue to remain arrested in length but widen to 8 – 15 µm as seen in Figure 4g.

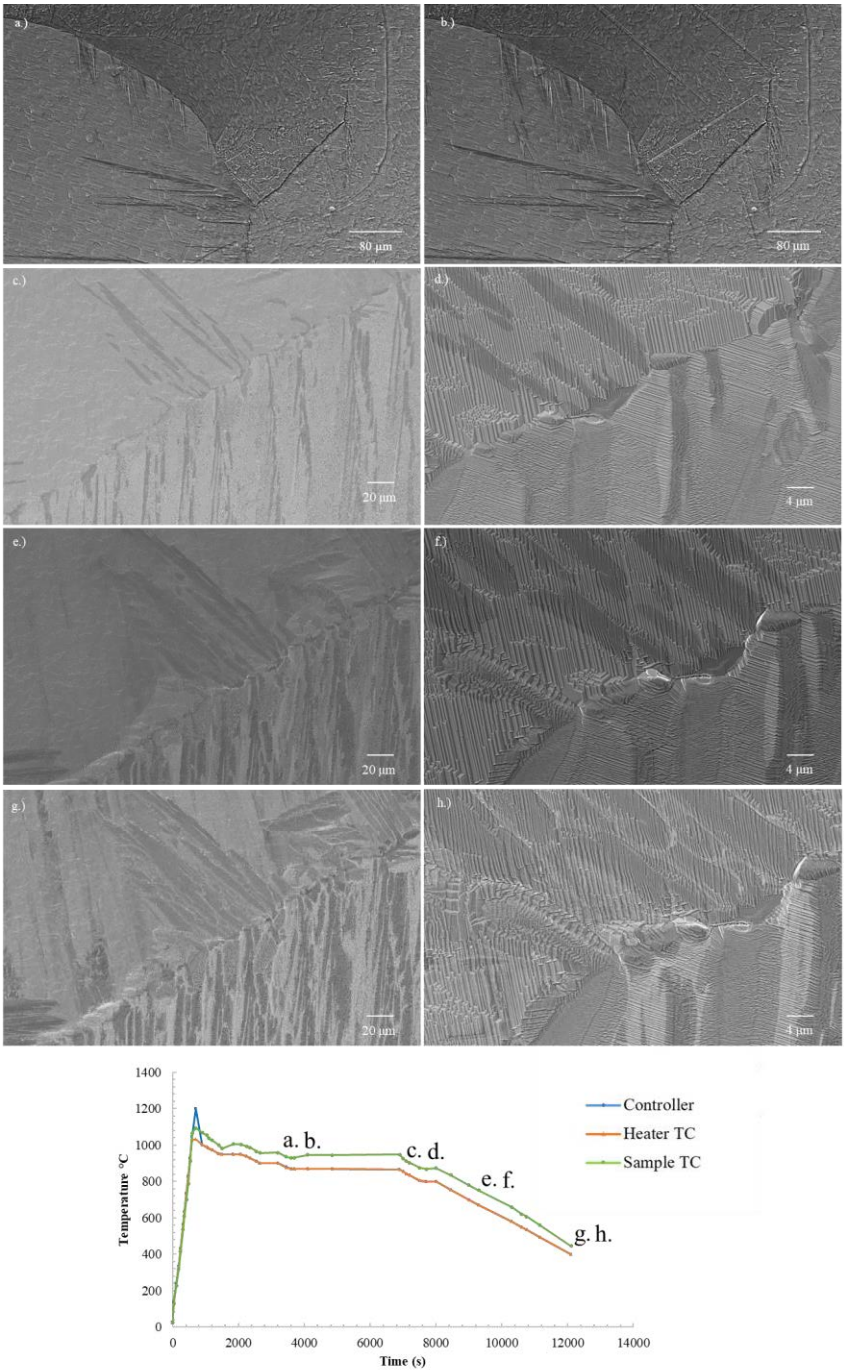

Figure 4: a) Initial lamellar microstructure formation upon cooling to 946 ° C. b) Lamellar microstructure after holding for two minutes at 946 °C; c&d) after holding for 45 min at 946 °C at low (c) and high (d) magnification; e) after cooling to 800 °C at 0.1 °C/s; f) after cooling to 835 °C (imaged just before Figure 4e); g&h) after cooling to 445 °C at

low (g) and high (h) magnification. Note: Figure 4a and 4b taken at 20 keV primary electron beam energy. Figure 4c-h taken at 5 keV. Temperature -time curve for this experiment included.

CONCLUSIONS:

Through in-situ annealing experiments in a scanning electron microscope, we were able to demonstrate the ability to image the developing microstructure of Ti 6% Al 4% V while cooling from above the β transus temperature. We observe the formation of surface topography above 930 ° C during heating, at which temperature α is observed to start rapidly dissolving into β. The observation of this surface topography and it's change in periodicity in lamellae regions may be an initial factor in the growth of lamellar/ acicular microstructures in surface regions.. Also, upon observing the growth of lamellar microstructures during cooling, we observe that the aspect ratio of the lamellae change for different cooling histories, giving rise to potential impacts on material property optimization.

ACKNOWLEDGMENTS:

This research is sponsored through grants from the National Science Foundation, Awards CMMI-1647005, and CMMI-1729336. This work was performed with the use of clean room and characterization facilities within the Center for Materials, Devices and Integrated Systems at Rensselaer Polytechnic Institute. We acknowledge collaborations with Dr. Dan Lewis, Dr. Antoinette Maniatty, Dr. John Wen, Arun Baskaran, Sagar Bhatt, Anant Kekre, Michael Allahua, Dr. Dustin Andersen, and the help and expertise of Kammrath and Weiss with equipment development.

References:

[1] A. Gomez-Gallegos, P. Mandal, D. Gonzalez, N. Zuelli, and P. Blackwell, "Studies on Titanium Alloys for Aerospace Application," *Defect Diffus. Forum*, vol. 385, pp. 419–423, 2018.

[2] D. Banerjee and J. C. Williams, "Perspectives on titanium science and technology," *Acta Mater.*, vol. 61, pp. 844–879, 2013.

[3] X. H. Shi, W. D. Zeng, C. L. Shi, H. J. Wang, and Z. Q. Jia, "The effects of colony microstructure on the fatigue crack growth behavior for Ti-6A1-2Zr-2Sn-3Mo-1Cr-2Nb titanium alloy," *Mater. Sci. Eng. A*, vol. 621, pp. 252–258, 2015.

[4] D. A. Porter, K. E. Easterling, and M. Y. Sherif, *Phase Transformations in Metals and Alloys, Third Edition*. 2009.

[5] S. L. Semiatin, V. Seetharaman, and I. Weiss, "Hot workability of titanium and titanium aluminide alloys—an overview," *Mater. Sci. Eng. A*, vol. 243, no. 1–2, pp. 1–24, 2002.

[6] G. Lütjering, "Influence of processing on microstructure and mechanical properties of (α+β) titanium alloys," *Mater. Sci. Eng. A*, vol. 243, no. 1–2, pp. 32–45, 1998.

[7] N. Poondla, T. S. Srivatsan, A. Patnaik, and M. Petraroli, "A study of the microstructure and hardness of two titanium alloys: Commercially pure and Ti-6Al-4V," *J. Alloys Compd.*, vol. 486, no. 1–2, pp. 162–167, 2009.

[8] S. L. Semiatin, S. L. Knisley, P. N. Fagin, F. Zhang, and D. R. Barker, "Microstructure evolution during alpha-beta heat treatment of Ti-6Al-4V," *Metall. Mater. Trans. A Phys. Metall. Mater. Sci.*, vol. 34, no. 10, pp. 2377–2386, 2003.

[9] S. Patil *et al.*, "Effect of α and β Phase Volume Fraction on Machining Characteristics of Titanium Alloy Ti6Al4V," *Procedia Manuf.*, vol. 6, pp. 63–70, 2016.

[10] B. J. Hayes *et al.*, "Predicting tensile properties of Ti-6Al-4V produced via directed energy deposition," *Acta Mater.*, vol. 130, no. July, pp. 120–133, 2017.

[11] S. Shademan, V. Sinha, A. B. O. Soboyejo, and W. O. Soboyejo, "An investigation of the effects of microstructure and stress ratio on fatigue crack growth in Ti-6Al-4V with colony α/β microstructures," *Mech. Mater.*, vol. 36, pp. 161–175, 2004.

[12] Y. Ma *et al.*, "Fatigue crack tip plastic zone of α + β titanium alloy with Widmanstatten microstructure," *J. Mater. Sci. Technol.*, vol. 34, no. 11, pp. 2107–2115, 2018.

[13] X. Zhang, F. Martina, J. Ding, X. Wang, and S. W. Williams, "Fracture toughness and fatigue crack growth rate properties in wire + arc additive manufactured Ti-6Al-4V," *Fatigue Fract. Eng. Mater. Struct.*, vol. 40, no. 5, pp. 790–803, 2017.

[14] K. S. Chan and D. A. Koss, "Fracture toughness of Widmanstatten colonies of an α-β titanium alloy," *Mater. Sci. Eng.*, vol. 43, no. 2, pp. 177–186, 1980.

[15] C. J. Boehlert, C. J. Cowen, S. Tamirisakandala, D. J. McEldowney, and D. B. Miracle, "In situ scanning electron microscopy observations of tensile deformation in a boron-modified Ti–6Al–4V alloy," *Scr. Mater.*, vol. 55, no. 5, pp. 465–468, 2006.

[16] E. Alabort, D. Putman, and R. C. Reed, "Superplasticity in Ti-6Al-4V: Characterisation, modelling and applications," *Acta Mater.*, vol. 95, pp. 428–442, 2015.

[17] D. A. Brice *et al.*, "Oxidation behavior and microstructural decomposition of Ti-6Al-4V and Ti-6Al-4V-1B sheet," *Corros. Sci.*, vol. 112, pp. 338–346, 2016.